Electronic Supplementary Information (ESI)

Tables

Table S1: Reported transmittance of solar radiation through the snowpack in different experiments. Note that the extinction coefficients calculated for each study refer to the wavelength range studied and hence are not directly comparable with each other or with the results from our study, but give only an indication for the rate of extinction in each case.

Wavelength Range and device	Extinction Coefficient (cm^{-1})	Peak Transmittance	Location	Snow Type (grain size)	Publication
broadband with a pyrheliometer /thermistors	0.112 fine snow 0.116 coarse snow (0-40 cm depth)	Not applicable	Sierra Nevada, California.	Fine crystal structure	Gerdel (1948)
420-650 nm (four wavelengths)	0.07-0.35 cm^{-1} (sensu Mantis 1951)	420 nm - Longer λ attenuated more	Maudheim, Norway	0.3 mm (modelled)	Lilljequist (1956) in Bohren & Barkstrom (1974)
400-730 nm at 50 nm res. spectroradiometer	0.132 at 35 cm depth in fresh snow, 0.023 at 200 cm depth old snow.	500 nm (fresh) 550 nm(old snow)	Franklin Basin Utah USA (2300 m asl)	Seasonal snow from fresh (March) to snow/ice (May)	Richardson & Salisbury (1977)
400-750 nm at 25nm res. 750-1050 nm 50 nm res. Scanning spectroradiometer	0.115 powder snow at 450nm (0-46 cm depth) 0.177 small crystals (0-16 cm depth)	450-600 nm peak 475 nm	Hoodo and Bachelor Butte, Oregon, USA	Powder snow 13th February, fine snow 15th May.	Curl Jr. et al., (1972)
400-730 nm 25 nm res. scanning spectroradiometer	0.109 at 450 nm at 69 cm depth	425-600 nm peak 550 nm	Franklin Basin, Utah (alpine 2300 m asl)	Seasonal snow measured on 26th February	Kimball et al., (1973)
350-900 nm (50-150 nm res.) silicon photodiode spectrometer	0.329 at 350 nm (2-12 cm depth)	450-500 nm (coarse scale)	McMurdo Sound, Antarctica	0.2 mm seasonal snow – removed for measurement	Beaglehole et al. (1998)
350-1050 nm (quantum sensor)	0.30 at 10 cm depth fresh snow, PAR	400 nm with a minor peak at	Brùggerhalvùya peninsula, Svalbard	Variable grain sizes >0.5mm	Gerland et al. (1999)

400-700 nm (FieldSpec FR spectrometer)	0.164 at 14 cm depth old snow, PAR 0.35 at 0-20 cm depth fresh snow 0.17 0-20 cm depth old snow	430 nm			Gerland et al. (2000)
310-400 nm (1 nm resolution) array spectrometer	0.32 (0-7.2 cm depth)	Flat (very small peak 345 nm)	Mars Oasis, Antarctica	Receding edge of seasonal snowpack ice/snow mix	Cockell & Cordobá-Jabonero (2004)
350-1000 nm 3nm res. scanning spectroradiometer	Highly variable (40-135 cm)	390 nm	Concordia, Antarctica	Permanent snow, old dense and rounded at depth >40 cm	Warren et al. (2006)
400-1000 nm 5 nm res. array spectrometer	0.23-(2-4 cm) 0.11 (7-12 cm) at 400 nm	450-500 nm peak (Wavelength dependent - longer attenuated faster)	Semi-controlled conditions – Hanover, New Hampshire	Various (0.3-1.0 mm)	Perovich (2007)
320-600 nm (1nm res. Six-probe array spectrometer)	Various 0.105 at 30 cm Table 2 of France et al., (2011)	440 nm peak	Concordia, Antarctica	Permanent, rounded crystals (0.3-0.5 mm)	France & King (2012)

Res. = Resolution

Conversion from gm cal m^{-2} to W m^{-2} (1 cal/ = 41867.28072 W m^{-2})

Table S2: Average spectral photon irradiance (µmol m^{-2} s^{-1}) given for spectral integrals, measured at 30 cm above the snow, at the snow surface (0 cm), and along a transect beneath the snow surface down to 24 cm depth (27-01-2019). Ratios of certain spectral integrals are given: the UV-B:PAR ratio and the UV-B:UV-A ratio report UV-B × 1000 to give readable results. Each wavelength range and the R:FR ratio are defined by Sellaro et al. (2010). The extinction coefficients (exp) of the fitted function (equation 1) are given to two alternative depths.

Depth (cm)	**PAR (PPFD)**	**UV-B**	**UV<350 (nm)**	**UV>350 (nm)**	**UV-A**	**Blue**	**Green**	**Red**	**Far-red**	**Infra-red (<900nm)**	**UVB:UVA (×1000)**	**UVB:PAR (×1000)**	**UVA:PAR ratio**	**R:FR ratio**	**B:G ratio**	**B:R ratio**
30 above	373.3	0.061	5.98	17.87	23.79	71.43	88.28	91.48	82.34	234.2	2.58	0.165	0.064	1.11	0.81	0.78
0	383.5	0.102	6.53	19.18	25.61	75.38	91.07	92.00	82.34	235.6	3.98	0.266	0.067	1.12	0.83	0.82
1	129.9	0.038	3.29	9.06	12.31	29.47	31.15	27.80	24.25	70.32	3.01	0.298	0.096	1.15	0.95	1.09
3	82.00	0.027	2.31	6.27	8.55	19.47	19.70	16.84	14.65	42.49	3.21	0.335	0.104	1.15	0.99	1.16
5	55.51	0.019	1.53	4.21	5.73	13.20	13.29	11.35	9.74	26.91	3.24	0.342	0.104	1.17	0.99	1.19
7	43.73	0.013	1.05	2.99	4.02	10.00	10.62	9.19	7.88	19.70	3.26	0.300	0.092	1.17	0.94	1.09
11	13.09	0.003	0.24	0.79	1.02	3.03	3.39	2.56	1.64	1.83	2.74	0.214	0.078	1.57	0.90	1.18
14	10.31	0.002	0.19	0.63	0.82	2.47	2.75	1.90	1.06	0.92	2.97	0.235	0.079	1.80	0.89	1.30
18	9.67	0.002	0.16	0.56	0.72	2.25	2.57	1.83	1.02	0.89	2.70	0.201	0.074	1.78	0.87	1.23
20	5.69	0.001	0.09	0.32	0.41	1.38	1.59	0.97	0.42	0.21	2.95	0.213	0.073	2.31	0.86	1.41
22	3.04	0.000	0.05	0.18	0.23	0.78	0.88	0.46	0.17	0.06	1.01	0.077	0.077	2.76	0.89	1.68
24	1.16	0.000	0.01	0.07	0.07	0.29	0.35	0.17	0.05	0.01	0.82	0.053	0.064	3.40	0.84	1.69
	Empirical Extinction Coefficients (µmol m^{-2} s^{-1} cm^{-1}; 0-5-cm depth)															
Exp	-0.350	-0.302	-0.279	-0.276	-0.317	-0.347	-0.378	-0.385	-0.392							
R^2	0.836	0.82	0.900	0.894	0.855	0.837	0.825	0.825	0.840							
	Empirical Extinction Coefficients (µmol m^{-2} s^{-1} cm^{-1}; 0-20-cm depth)															
-Exp	-0.194	-0.211	-0.193	-0.192	-0.191	-0.191	-0.217	-0.259	-0.364							
R^2	0.94	0.96	0.95	0.96	0.94	0.93	0.94	0.95	0.96							

Figures

Fig. S1. Photograph of (A) the diffusor covered by 1-cm snow and (B) the measuring set-up in the field prior to measurements through the snow pack (note that for actual measurements just the diffuser – and attached optical fibre - were inserted into the snow)

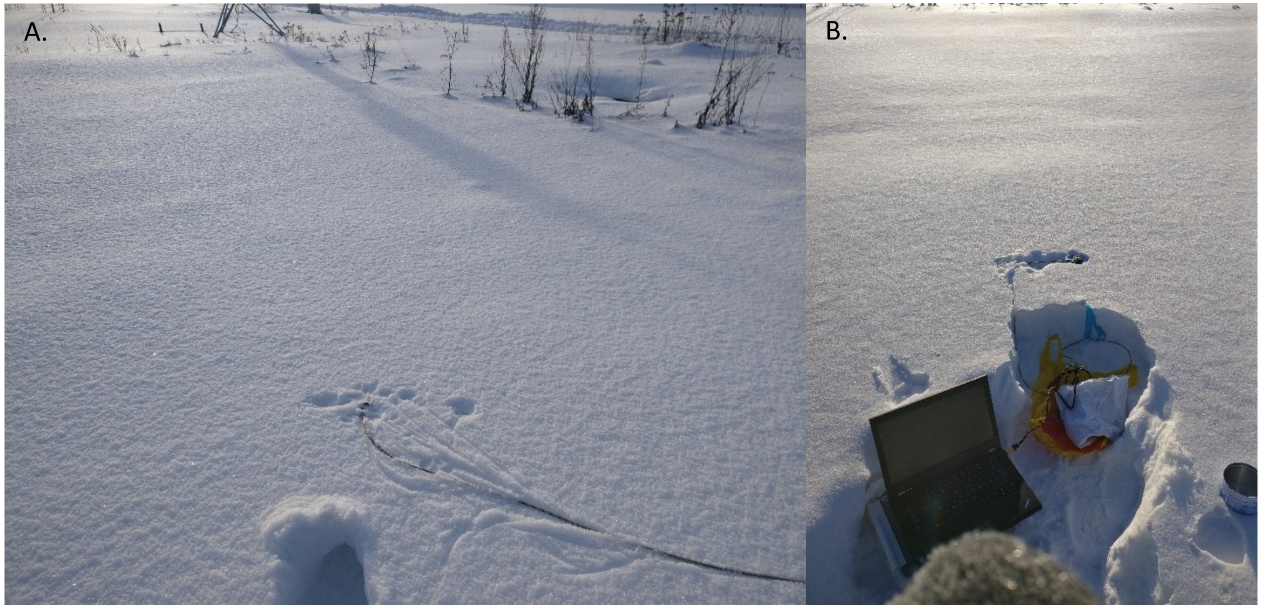

Fig. S2. Comparison of measured spectral irradiance at 30-cm above the snow and spectral irradiance modelled using libradtran (Emde et al. 2016) following Brelsford (2016) for 28-02-2018. Solar azimuth 203.05°, solar elevation 19.83°, and cosine of zenith angle 0.3392°.

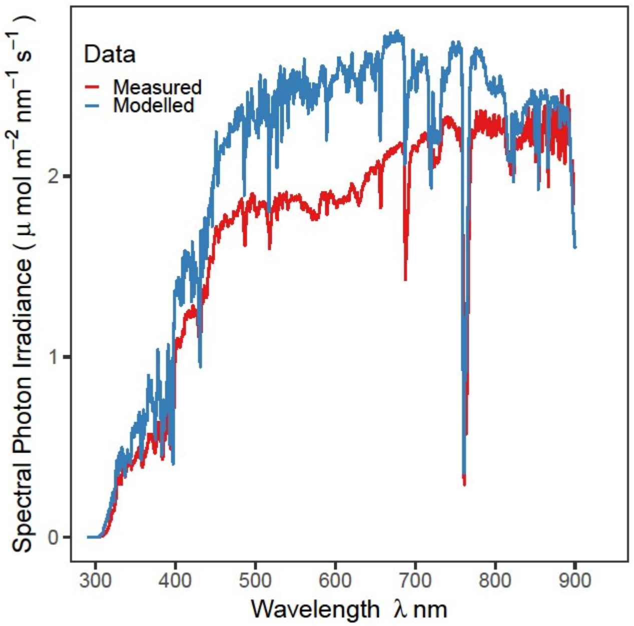

Fig. S3: Detail from Fig. 2 plotted on a $\log_{10}$ axis for the UV-region of the spectrum (305 nm – 400 nm are plotted).

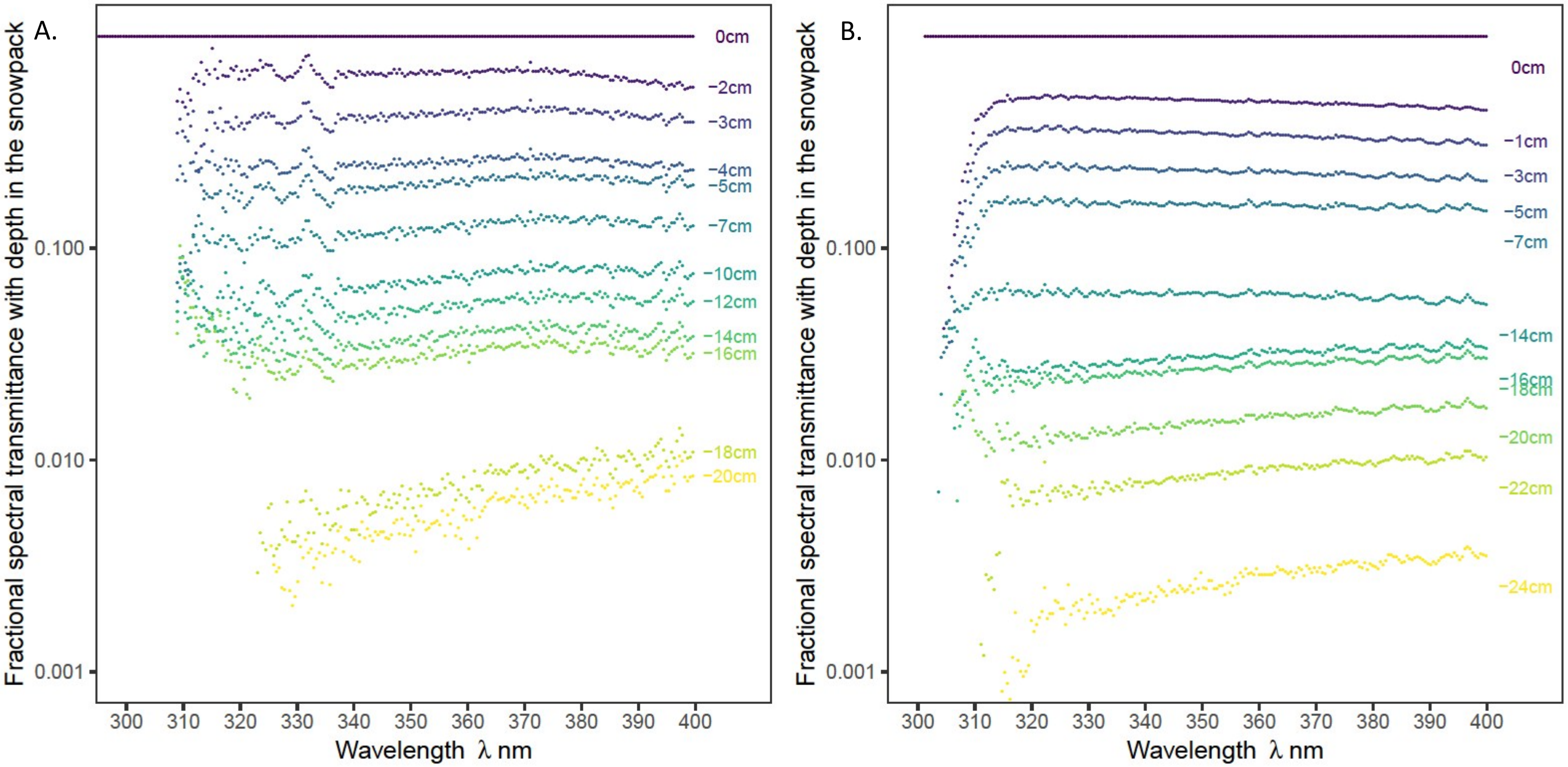

Fig. S4: Plots of the relationships of spectral integrals with snow depth on dates (A.) 2018-02-28 and (B.) 2019-01-27. Photosynthetically Active Radiation (PAR: 400-700 nm) is plotted on the primary axis, and unweighted UV-A (315-400 nm) and UV-B (280-315 nm) radiation on the secondary axis. At very low irradiances readings are unreliable so the UV-B line is fitted only to 12-cm depth. (C.) PAR on 2018-02-28 and (D.) 2019-01-27 broken down into blue (420-490 nm), green (500-570 nm) and red (620-680 nm), and far-red (700-750 nm) regions, plotted and with fitted lines (equation 1) in their respective colours (defined according to Sellaro et al., 2010) and exp in units (µmol m^{-2} s^{-1} cm^{-1}).

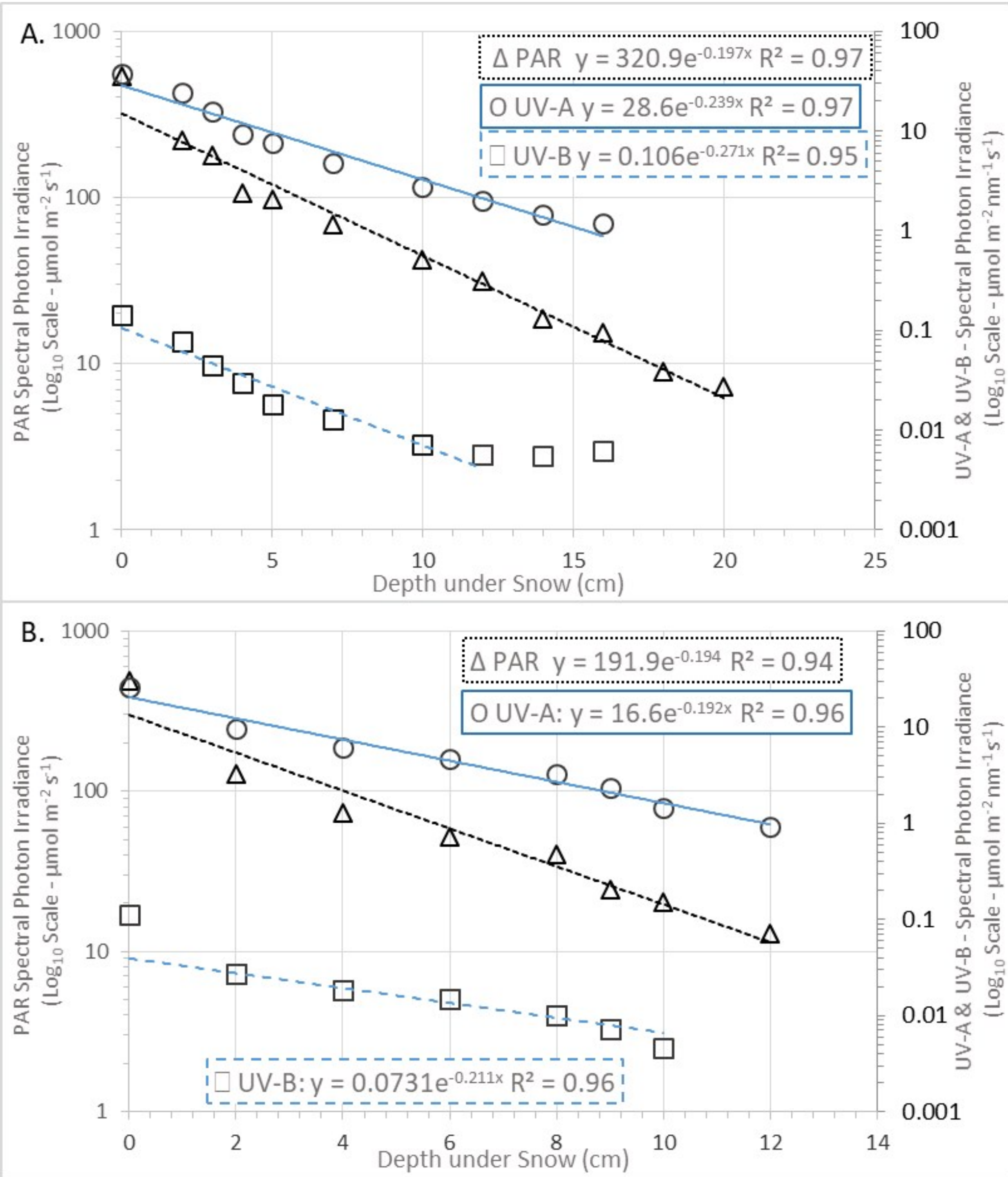

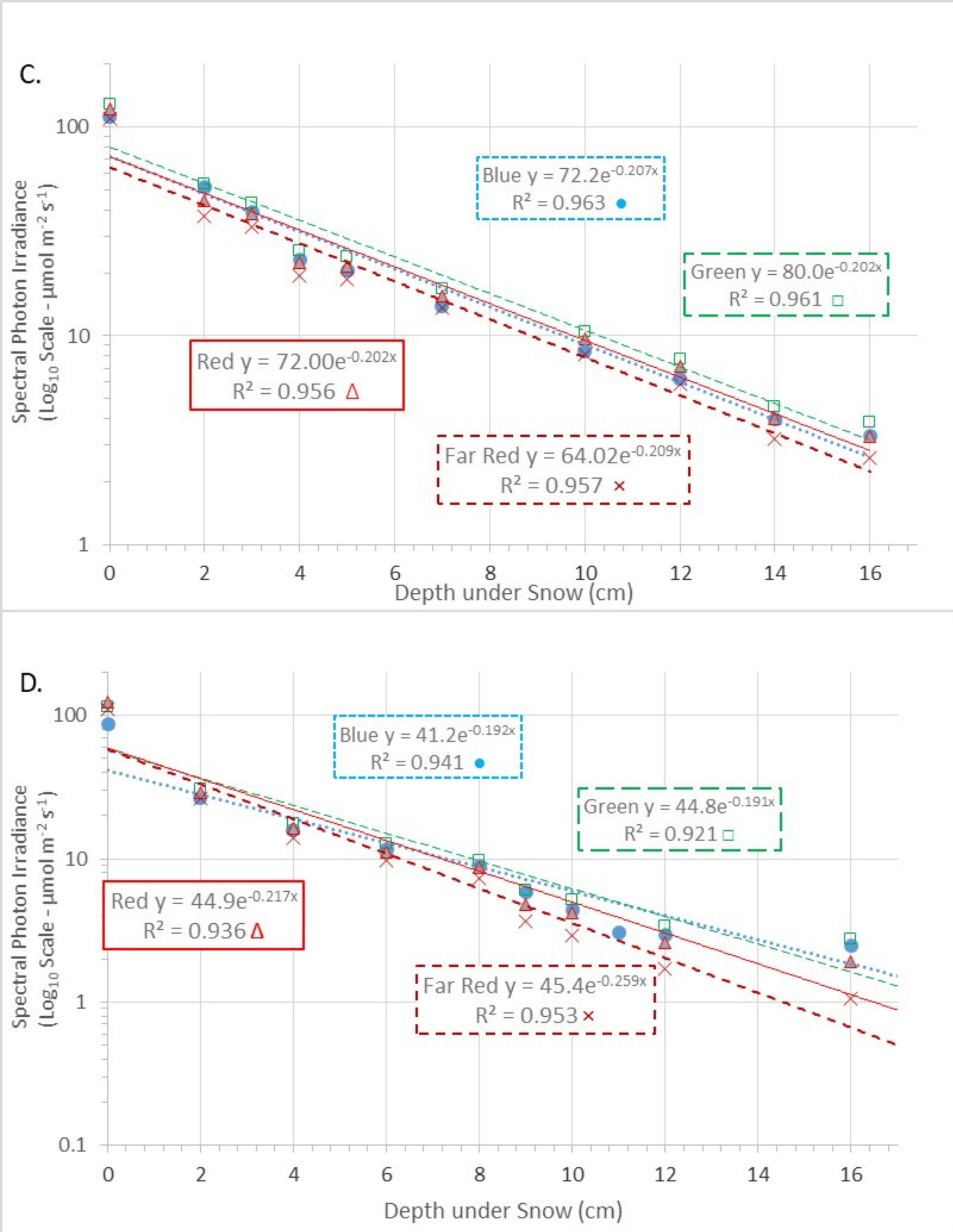
C.
Spectral Photon Irradiance (Log10 Scale - µmol m-2 s-1)
100
10
1
0
2
4
6
8
10
12
14
16
Depth under Snow (cm)
Blue y = 72.2e-0.207x
R² = 0.963
Green y = 80.0e-0.202x
R² = 0.961
Red y = 72.00e-0.202x
R² = 0.956
Far Red y = 64.02e-0.209x
R² = 0.957
D.
Spectral Photon Irradiance (Log10 Scale - µmol m-2 s-1)
100
10
1
0.1
0
2
4
6
8
10
12
14
16
Depth under Snow (cm)
Blue y = 41.2e-0.192x
R² = 0.941
Green y = 44.8e-0.191x
R² = 0.921
Red y = 44.9e-0.217x
R² = 0.936
Far Red y = 45.4e-0.259x
R² = 0.953

Fig. S5: Plots of the change ratios of spectral integrals with snow depth on each of the measurement dates. (A.) Photon ratio of unweighted UV-A radiation to PAR. (B.) Photon ratio of blue (420-490 nm) to green (500-570 nm) irradiance. (C.) The UV-B-to-UV-A photon ratio.

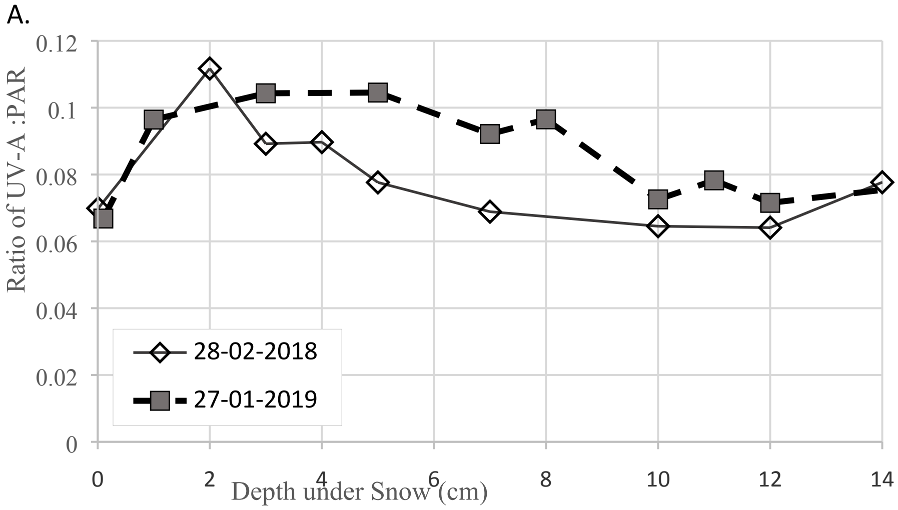

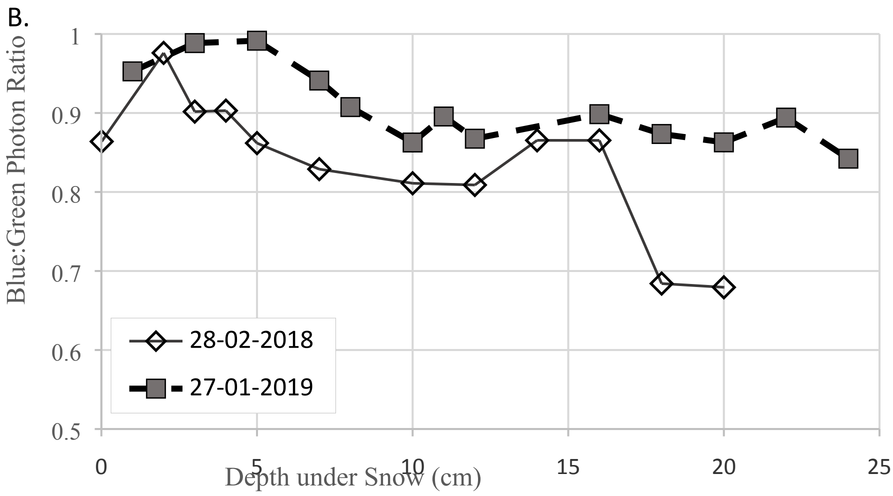

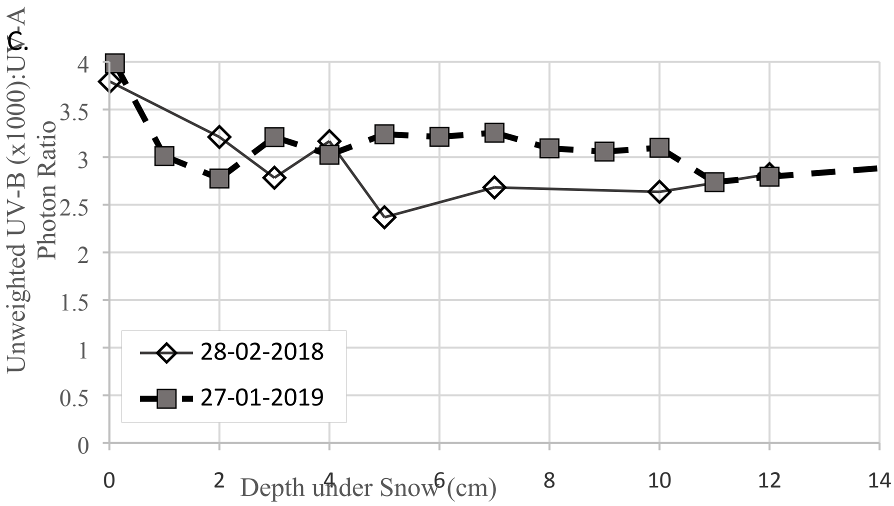

Fig. S6: Hemispherical photograph taken at the location of the measurements of the snowpack. South is upper-most on the photo. The nearest vegetation was a copse of birch *c* 50 m to the north, otherwise no building or vegetation were within 100 m.

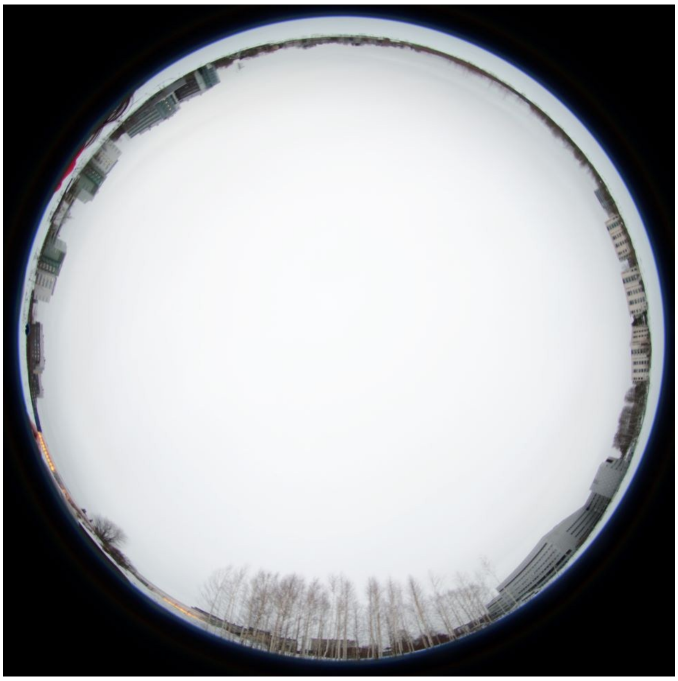

Reference List ESM

Beaglehole D, Ramanathan B, Rumberg J. (1998), The UV to IR transmittance of Antarctic snow. *J Geophysical Research,* **103**, 8849-8857.

Bohren CF, Barkstrom BR. (1974), Theory of the optical properties of snow. *Journal of Geophysical Research* **79**, 4527-4535.

Brelsford CC. (2016) Radiative transfer theory and modelling with libRadtran. *UV4Plants Bulletin*, **2016**, 45-50.

Cockell CS, Cordobá-Jabonero C. (2004) Coupling of Climate Change and Biotic UV Exposure Through Changing Snow-Ice Covers in Terrestrial Habitats. *Photochem. Photobiol. Sci*, **79**, 26-31

Curl Jr. H, Hardy JT, Ellermeier R. (1972) Spectral Absorption of Solar Radiation in Alpine Snowfields. *Ecology*, **53**, 1189-1194.

Emde C, Buras-Schnell R, Kylling A, Mayer B, Gasteiger J, Hamann U, Kylling J, Richter B, Pause C, Dowling T and Bugliaro L, (2016), The libRadtran software package for radiative transfer calculations (version 20 1), *Geosci Model Dev,* **9**, 1647-1672.

France JL, King MD, Frey MM, Erbland J, Picard G, Preunkert A, MacArthur A, Savarino J. (2011) Snow optical properties at Dome C (Concordia), Antarctica; implications for snow emissions and snow chemistry of reactive nitrogen. *Atmos. Chem. Phys,* **11**, 9787–9801.

France JL, King MD. (2012) The effect of measurement geometry on recording solar radiation attenuation in snowpack (e-folding depth) using fibre-optic probes. *Journal of Glaciology*, **58**, 417-418.

Gerdel RW, (1948) Penetration of radiation into the snow pack. *Transactions of the American Geophysical Union,* **29**, 366-374.

Gerland S, Winther J-G, Obaek JB, Liston GE, Oritsland NA, Blanco A, Ivanov B, (1999) Physical and optical properties of snow covering Arctic tundra on Svalbard. *Hydrological Processes*, **13**, 2331-2343.

Gerland S, Liston GE, Winther J-G, Orbaek JB, Ivanoc BV. (2000) Attenuation of solar radiation in Arctic snow: field observations and modelling *Annals of Glaciology*, **31**, 363-368.

Kimball SL, Bennett BD, Salisbury FB. (1973), Growth and Development of Montane Species at Near-Freezing Temperatures, *Ecology*, **54**, 168-173.

Lilljequist, GH. (1956) *Energy exchange of an Antarctic snow-field, shortwave radiation (420-650 nm, Maudheim 70°03'S, 10°56'W), Norwegian-British-Swedish Antarctic Expedition*, **1,** 949-952, Scientific Results,2 part IA, Norsk Polarinstitutt, Oslo, Norway, 1956.

Perovich DK. (2007) Light reflection and transmission by a temperate snow cover. *Journal of Glaciology* **53**, 201-211.

Richardson SG, Salisbury FB. (1977) Plant responses to the light penetrating snow. *Ecology,* **58**, 1152-1158.

Sellaro R, Crepy M, Trupkin SA, Karayekov E, Buchovsky AS, Rossi C, Casal JJ. (2010). Cryptochrome as a sensor of the blue/green ratio of natural radiation in Arabidopsis. *Plant Physiology*, **154**, 401-409. doi:10.1104/pp.110.160820.

Warren SG, Brandt RE, Grenfell TC. (2006) Visible and near-ultraviolet absorption spectrum of ice from transmission of solar radiation into snow. *Applied Optics,* **45**, 5320-5335.